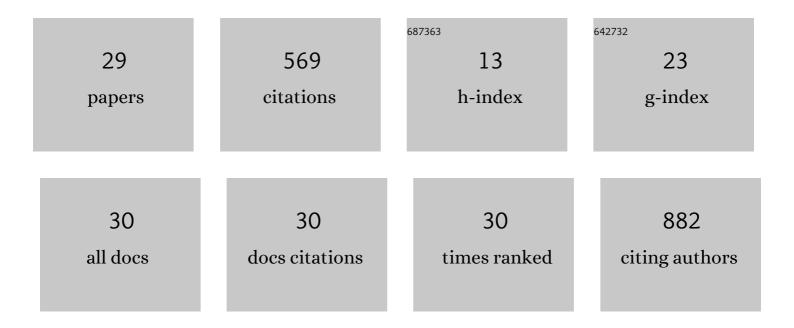
Jan Garrevoet

List of Publications by Year in descending order

Source: https://exaly.com/author-pdf/1771002/publications.pdf Version: 2024-02-01



#	Article	IF	CITATIONS
1	Perfect X-ray focusing via fitting corrective glasses to aberrated optics. Nature Communications, 2017, 8, 14623.	12.8	134
2	Fast X-ray microfluorescence imaging with submicrometer-resolution integrating a Maia detector at beamline P06 at PETRAâ€III. Journal of Synchrotron Radiation, 2016, 23, 1550-1560.	2.4	49
3	Methodology toward 3D Micro X-ray Fluorescence Imaging Using an Energy Dispersive Charge-Coupled Device Detector. Analytical Chemistry, 2014, 86, 11826-11832.	6.5	36
4	Incremental distribution of strontium and zinc in great ape and fossil hominin cementum using synchrotron X-ray fluorescence mapping. Journal of the Royal Society Interface, 2018, 15, 20170626.	3.4	36
5	Radiation Doseâ€Enhancement Is a Potent Radiotherapeutic Effect of Rareâ€Earth Composite Nanoscintillators in Preclinical Models of Glioblastoma. Advanced Science, 2020, 7, 2001675.	11.2	36
6	Salinity and dissolved organic carbon both affect copper toxicity in mussel larvae: Copper speciation or competition cannot explain everything. Environmental Toxicology and Chemistry, 2015, 34, 1330-1336.	4.3	30
7	Synchrotron X-ray fluorescence mapping of Ca, Sr and Zn at the neonatal line in human deciduous teeth reflects changing perinatal physiology. Archives of Oral Biology, 2019, 104, 90-102.	1.8	28
8	PtyNAMi: ptychographic nano-analytical microscope. Journal of Applied Crystallography, 2020, 53, 957-971.	4.5	25
9	Development and Applications of a Laboratory Micro X-ray Fluorescence (μXRF) Spectrometer Using Monochromatic Excitation for Quantitative Elemental Analysis. Analytical Chemistry, 2015, 87, 6544-6552.	6.5	21
10	Hard X-ray wavefront correction via refractive phase plates made by additive and subtractive fabrication techniques. Journal of Synchrotron Radiation, 2020, 27, 1121-1130.	2.4	19
11	Probing Intracellular Element Concentration Changes during Neutrophil Extracellular Trap Formation Using Synchrotron Radiation Based X-Ray Fluorescence. PLoS ONE, 2016, 11, e0165604.	2.5	17
12	A Standalone, Batteryâ€Free Light Dosimeter for Ultraviolet to Infrared Light. Advanced Functional Materials, 2022, 32, .	14.9	17
13	Nanofocusing with aberration-corrected rotationallyÂparabolic refractive X-ray lenses. Journal of Synchrotron Radiation, 2018, 25, 108-115.	2.4	16
14	Fast XANES fluorescence imaging using a Maia detector. Journal of Synchrotron Radiation, 2018, 25, 892-898.	2.4	12
15	Four-Fold Multi-Modal X-ray Microscopy Measurements of a Cu(In,Ga)Se2 Solar Cell. Materials, 2021, 14, 228.	2.9	12
16	Synchrotron X-ray fluorescence imaging of strontium incorporated into the enamel and dentine of wild-shot orangutan canine teeth. Archives of Oral Biology, 2020, 119, 104879.	1.8	11
17	Upscaling of multi-beam x-ray ptychography for efficient x-ray microscopy with high resolution and large field of view. Applied Physics Letters, 2021, 118, .	3.3	11
18	Multi-beam X-ray ptychography using coded probes for rapid non-destructive high resolution imaging of extended samples. Scientific Reports, 2022, 12, 6203.	3.3	9

Jan Garrevoet

#	Article	IF	CITATIONS
19	Salinity, dissolved organic carbon, and interpopulation variability hardly influence the accumulation and effect of copper in <i>Mytilus edulis</i> . Environmental Toxicology and Chemistry, 2017, 36, 2074-2082.	4.3	8
20	Growth and development of the third permanent molar in Paranthropus robustus from Swartkrans, South Africa. Scientific Reports, 2020, 10, 19053.	3.3	7
21	Determination of the through-plane profile of vanadium species in hydrated Nafion studied with micro X-ray absorption near-edge structure spectroscopy – proof of concept. Journal of Synchrotron Radiation, 2021, 28, 1865-1873.	2.4	6
22	Ptychographic Nano-Analytical Microscope (PtyNAMi) at PETRA III: signal-to-background optimization for imaging with high sensitivity. , 2019, , .		5
23	Sub-micrometer focusing setup for high-pressure crystallography at the Extreme Conditions beamline at PETRAâ€III. Journal of Synchrotron Radiation, 2022, 29, 654-663.	2.4	5
24	Scanning Hard X-Ray Microscopy Based on Be CRLs. Microscopy and Microanalysis, 2018, 24, 188-189.	0.4	4
25	Micro x-ray fluorescence analysis of trace element distribution in frozen hydrated HeLa cells at the P06 beamline at Petra III. Biointerphases, 2021, 16, 011004.	1.6	4
26	Tracking dynamic structural changes in catalysis by rapid 2D-XANES microscopy. Journal of Synchrotron Radiation, 2021, 28, 1518-1527.	2.4	4
27	Spatial Distribution of Intracellular Ion Concentrations in Aggregateâ€Forming HeLa Cells Analyzed by μâ€XRF Imaging. ChemistryOpen, 2022, 11, e202200024.	1.9	4
28	Comparison of XBIC and LBIC measurements of a fully encapsulated c-Si solar cell. , 2021, , .		3
29	Incremental Elemental Distribution in Chimpanzee Cellular Cementum: Insights from Synchrotron X-Ray Fluorescence and Implications for Life-History Inferences. , 2022, , 138-154.		Ο